Earth Science Informatics
https://doi.org/10.1007/s12145-020-00541-x

RESEARCH ARTICLE

Predicting and mapping land cover/land use changes in Erbil /Iraq using CA-Markov synergy model

Nabaz R. Khwarahm[1] · Sarchil Qader[2,3] · Korsh Ararat[4] · Ayad M. Fadhil Al-Quraishi[5]

Received: 1 June 2020 / Accepted: 23 October 2020

Abstract

One of the most dynamic components of the environment is land use land cover (LULC), which have been changing remarkably since after the industrial revolution at various scales. Frequent monitoring and quantifying LULC change dynamics provide a better understanding of the function and health of ecosystems. This study aimed at modelling the future changes of LULC for the Erbil governorate in the Kurdistan region of Iraq (KRI) using the synergy Cellular Automata (CA)-Markov model. For this aim, three consecutive-year Landsat imagery (i.e., 1988, 2002, and 2017) were classified using the Maximum Likelihood Classifier. From the classification, three LULC maps with several class categories were generated, and then change-detection analysis was executed. Using the classified (1988–2002) and (2002–2017) LULC maps in the hybrid model, LULC maps for 2017 and 2050 were modelled respectively. The model output (modelled 2017) was validated with the classified 2017 LULC map. The accuracy of agreements between the classified and the modelled maps were $K_{no} = 0.8339$, $K_{location} = 0.8222$, $K_{standard} = 0.7491$, respectively. Future predictions demonstrate between 2017 and 2050, built-up land, agricultural land, plantation, dense vegetation and water body will increase by 173.7% (from 424.1 to 1160.8 km^2), 79.5% (from 230 to 412.9 km^2), 70.2% (from 70.2 to 119.5 km^2), 48.9% (from 367.2 to 546.9 km^2) and 132.7% (from 10.7 to 24.9 km^2), respectively. In contrast, sparse vegetation, barren land will decrease by 9.7% (2274.6 to 2052.8 km^2), 18.4% (from 9463.9-7721 km^2), respectively. The output of this study is invaluable for environmental scientists, conservation biologists, nature-related NGOs, decision-makers, and urban planners.

Keywords CA-Markov · Change-detection · Prediction · Classification · Remote sensing · GIS

Introduction

Land use and land cover changes have been shown to have a direct impact on the local, global environment, land degradation, and climate, which in turn reduces ecosystem services and functions (Karki et al. 2018; Tolessa et al. 2017). The intensity, speed, and degree of LULC changes are now faster compared to the past because of the development of society, and the rapid increase in population resulted in disturbing a large number of landscapes on Earth (Lambin and Meyfroidt 2011). For instance, at least 50% of Earth's ice-free land surface of the planet transformed by human actions (Hooke et al. 2012). Annually, 12 million hectares of agricultural land are lost (23 ha/min) because of drought and desertification, where 20 million tons of grain could have been grown (UN SDG 2020). On the global scale, urban land area increased by 346.4 thousand km^2 and growth by 1.3% from 1992 to 2016 (He et al. 2019). In addition, considering the current trends in population density change, by 2030, the urban land cover will increase by 1.2 million km^2 (Seto et al. 2012). Therefore, estimating current and future LULC changes can be essential to the decision making of environmental management and future planning.

✉ Nabaz R. Khwarahm
khwarahm21302@alumni.itc.nl

[1] Department of Biology, College of Education, University of Sulaimani, Sulaimani, Kurdistan Region, Iraq

[2] WorldPop, Geography and Environmental Science, University of Southampton, Southampton, UK

[3] Natural Resources Department, College of Agricultural Engineering Sciences, University of Sulaimani, Sulaimani, Kurdistan Region, Iraq

[4] Department of Biology, College of Science, University of Sulaimani, Sulaimani, Kurdistan Region, Iraq

[5] Surveying and Geomatics Engineering Department, Faculty of Engineering, Tishk International University, Erbil 44001, Kurdistan Region, Iraq

Published online: 27 October 2020

With the development of satellite sensors, there has been increasing interest in using satellite remote sensing data for monitoring land use/land cover changes due to its ability to provide frequent data at different spatial and temporal coverage. Such characteristics have made the remote sensing data critical input to the LULC classification and change detection models. In this regard, Landsat image has been widely utilized to study LULC changes because of its free access to four decades of earth observation data and relatively high spatial resolution (Gómez et al. 2016; Li et al. 2020; Pflugmacher et al. 2019; Zhu and Woodcock 2014). Markov model and cellular automata (CA) have potential benefits in the study of land use changes. Although the Markov model has been widely used for land use changes, with its traditional version, it is challenging to predict the spatial pattern of land use changes. However, the spatial variation of LULC changes can be simulated more efficiently if the CA model with powerful spatial computing can be incorporated. The CA-Markov model is a robust and convenient approach in spatial and temporal dynamic modelling of LULC changes since it has the ability to incorporate both remote sensing and geographic information system (GIS) data efficiently (Hyandye and Martz 2017; Kamusoko et al. 2009; Singh et al. 2015). Numerous previous studies have successfully examined the simulation of the spatial-temporal change patterns of LULC using the CA Markov model (Fu et al. 2018; Hishe et al. 2020; Muller and Middleton 1994; Munthali et al. 2020). For instance, in China, the CA model was employed to predict the spatial pattern of land use in 2020 and 2036 in which the results can be used as a basis for development planning in Jiangle County (Naboureh et al. 2017). Parsa et al. (2016) successfully simulated the spatial pattern of Land use of 2036 in Arasbaran, Iran, and indicated that despite its usefulness in land use design, the model could be used as an early warning system. In Nepal, the CA-Markov model was compared to the GEOMOD model to predict future LULC changes in Phewa Lake Watershed, and it found that the integration of the Markov model and CA were effective in projecting future LULC scenarios (Regmi et al. 2017). Therefore, considering the vast application of the model in this field and its ability to widen understanding about the complexity of components of the spatial system, this work adopted the CA-Markov model to predict future LULC changes for Erbil governorate in Iraq.

Over the last decades, LULC in Iraq as a whole has been negatively affected by both anthropogenic and natural events. In particular, the country has been subjected to several anthropogenic and natural disturbances such as war and drought over the last few decades resulting in vast LULC changes. For instance, it has been estimated that 100,000 ha are lost on average annually due to land degradation (UN 2013). Meanwhile, an accurate estimation of LULC in Erbil and Iraq is not existent, and the official Iraqi government statistics may be unreliable (USDA 2008). However, several researchers have conducted remotely sensed based classification approaches to estimate LULC types at regional and sub-regional levels in the country. For example, a phenology based classification approach was developed by Qader et al. (2016) to map the dominant vegetation land cover types annually over Iraq; such as grassland, shrubland, and cropland, with an overall accuracy >85% from 2002 to 2012. Gibson et al. (2015) used Landsat satellite data to investigate the impact of three decades of continuous war and instability on central cultivated areas in Iraq, and the results revealed that the largest increase in cultivated area (20%) was detected during the period of United Nations sanctions (1990 to 2003). Other works focused on local areas, including Landsat dataset were used to investigate LULC changes in Sulaymaniyah (Alkaradaghi et al. 2018), the impacts of LULC changes on land surface temperature in Dohuk city (Faqe Ibrahim 2017), environmental degradation for Basra province was assessed using Landsat data (Hadeel et al. 2010), remote sensing data were used to assess the LULC changes in Karbala city (Mohammed et al. 2018). Almost all the previous works in the country have focused on current or past LULC changes, and based on our knowledge, there have been limited studies (Hadi et al. 2014; Omar et al. 2014) on prediction of spatial future LULC changes in Iraq. Therefore, this study aims to model the future changes of LULC for the Erbil governorate (seven administrative districts) in the Kurdistan region of Iraq (KRI) using the synergy Cellular Automata (CA)-Markov model.

Materials and methods

Study area

Erbil governorate is located in the north-east of the Republic of Iraq. It sits within the latitudes 35.33951° - 37.28115° N and longitudes 43.42642°- 44.79698° E. Erbil city is the political and economic capital of the KRI (https://gov.krd/english/). The area of Erbil governorate is around 15,214 km^2 (http://bot.gov.krd/erbil-province) with seven administrative districts (Fig. 1). The governorate has a semi-arid continental climate with very hot summer and cool, wet winter; sometimes, the maximum temperature reaches 42.2 °C in summer. Annual average maximum and minimum temperatures could range between 25.2 °C -13.9 °C, respectively. The Erbil governorate's northern and eastern parts are generally mountainous areas (Choman, Soran, and Mergasur). Thus, the annual rainfall is significantly higher than the plain western and southern parts (375-724 mm) (https://gov.krd/english/). The elevation in the mountainous areas can reach up to 3500 m above the sea level. Ecologically, Erbil is within the moist steppe zone (Guest 1966). Zagros Mountains forest-steppe and the Middle East Steppe Eco-region, which is

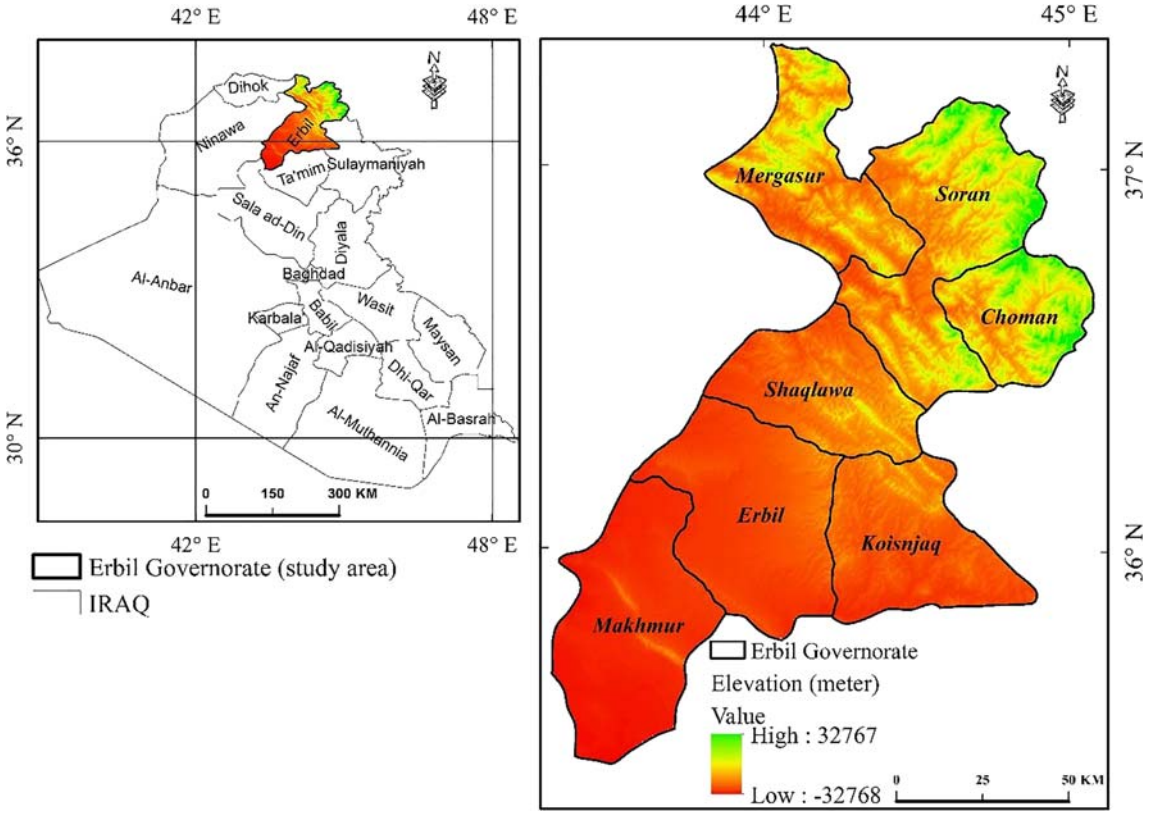

Fig. 1 Location map of the study site

mostly covered by grasses and herbs, also riverine woodlands/shrublands and wetland areas are existing within the area (https://www.worldwildlife.org/).

Dataset

The data used in this study are composed of three historic consecutive-year (1988, 2002, and 2007) Landsat satellite imagery with a spatial resolution of 30 m (Table 1). The imagery scenes with the least cloud cover percentage were downloaded from the United States Geological Survey (USGS) Earth Explorer portal (https://earthexplorer.usgs.gov).

Dataset pre-processing and classification

Before employing the classification procedure, the images were corrected from radiometric and atmospheric noises using Fast Line-of-sight Atmospheric Analysis of Hypercubes (FLAASH) settings of the ENVI 5.2 platform. Coefficients obtained from the metadata of the images were used in the setting. Radiometric and atmospheric corrections are required for deriving accurate quantitative surface information from satellite imagery (Liang et al. 2002).

Imagery scenes of the same time window and year were mosaicked, and the study area was extracted. Then, different band combinations, for example, RGB4,3,2 for TM and RGB5,4,3 for OLI were displayed to accurately identify surface features before generating training data or spectral signature data for the classification. Historical and current expert knowledge on the physiography of the study site, together with useful ancillary data, was taken into consideration when delineating the prospect feature classes based on the training samples.

For each LULC class identified, namely: dense vegetation, sparse vegetation, agricultural land, agricultural fallow, plantation, built-up area, barren land, and waterbody (Table 2),

Table 1 Sensor and date/time of the scene acquisitions from Landsat 5 Thematic Mapper (TM) and Landsat 8 (OLI_TIRS)

Path	Row	Date/time (Sensor)	Date/time (Sensor)	Date/time (Sensor_OLI_TIRS)
168	35	21.07.1988 (TM)	28.07.2002 (TM)	21.07.2017 (OLI)
168	36	21.07.1988 (TM)	28.07.2002 (TM)	21.07.2017 (OLI)
169	34	28.07.1988 (TM)	03.07.2002 (TM)	28.07.2017 (OLI)
169	35	28.07.1988 (TM)	03.07.2002 (TM)	28.07.2017 (OLI)

Table 2 Description of the LCLU classes

Class	Description
Dense vegetation	Very densely vegetated areas, mostly forest and dense shrublands.
Sparse vegetation	Scattered thin mixed forest areas, shrublands, and grassland patches.
Agricultural land	Currently cropped land with obvious greenness.
Agricultural fallow	Clearly visible croplands in the imagery, but no crops at the current time. Distinctive geometry for cropland is obvious.
Plantation	Densely vegetated areas but following a definite pattern, man-made forests and green spaces
Built-up area	Settlements: Artificial Infrastructure
Barren land	Lands with no obvious/or minimal vegetation, especially no obvious patches of trees or shrubs. Bare rocks, hills, soil, wasteland, rocky mounts and bare open lands.
Waterbody	Water bodies: any water bodies, e.g., rivers, fishponds, lakes, streams.

around 200 spectral signature (training samples) in the format of small polygons were extracted from the mosaicked images for each target year (Congalton and Green 2019). Employing the spectral signatures, maximum likelihood classifier (Richards and Richards 1999) was applied to classify the image of each consecutive year. In turn, three LULC maps at 30 m spatial resolution were generated. Maximum likelihood classification is based on the probability of a specific pixel belonging to an aggregate of similar or alike pixels (i.e., having similar/alike spectral distributions).

Classification assessment and change analysis

It is imperative to assess the degree of relationship or agreement between automated classification data with references/ground data (Congalton and Green 2019). An independent dataset constituting 30% of the training dataset for each class (i.e., 30% of the 200 spectral signature sample for each feature class is 60 points) was established (Foody 2002) within a GIS environment using ArcMap 10.3. That dataset was employed to assess the accuracy of 1988, 2002, and 2017 LULC maps resulted from the maximum likelihood classification. For doing this, an equalizing random sampling technique was designed by generating 480 points spreading across each LULC map for each year. The 480 random points represent 60 points per class for the classified data (Stehman and Czaplewski 1998). The points, for each target year, were then exported as shape files into Google Earth's historical imagery (i.e. reference layout) to be identified and labelled. The labelled points were then exported back to ArcMap to establish an error matrix with classified data (Rosenfield 1986; Van Oort 2007). From the error matrix, several statistical indices were calculated; for example, producer accuracy, user accuracy, and overall Kappa index of agreement.

After assessing the accuracy of the generated LULC maps between 1988 and 2017, the quantification of the dynamics of changes over time was investigated by calculating the area of specific class category per time window (i.e., for each target year 1988, 2002, and 2017) (Butt et al. 2015). Change detection was performed by comparing the status of certain class category pixels with subsequent class category pixels (cross-tabulation) (Jensen 1996; Pontius Jr and Cheuk 2006).

CA-Markov models

Markov model

Estimating the rate of change from one phase to another phase over space and time in spatial data is important for predicting future change scenarios (Takada et al. 2010). Markov chain model is one of the widely accepted models to quantify the magnitude of change over time by working out the transition probability matrix, transition area matrix of two LULC time-period maps (i.e., between t_0 and t_1). From these matrices, several conditional probability class categories, based on their pixel-wise status, are estimated (Eastman 2003; Houet and Hubert-Moy 2006).

CA model

The Markov model is proven efficient in simulating the status of change in LULC change detection studies (Biswas et al. 2019; López et al. 2001; Muller and Middleton 1994). However, the Markov model has a limitation in simulating the spatial allocation and distribution of the class categories in the LULC maps (Eastman 2012). On the other hand, the Cellular Automata (CA) model (Wolfram 1984) fills the gap of the spatial dimension limitation. The CA model assumes the status of a grid-cell is dependent on the dynamics of the cell itself and the surrounding grid-cells (Yang and Li 2007). The dynamics of the dependency could be simple and complex (i.e., linear and nonlinear). In other words, based on predefined transition conditions over time, the model predicts the new status of LULC class category based on the previous

status of LULC and those of its neighboring class categories (Guan et al. 2011; He et al. 2014; Liping et al. 2018).

Markov-CA synergy model

Markov chain model integrated with the CA model, provides a unique opportunity to predict and simulate LULC changes in both space and time consistently. This synergy model is efficient in simulating and predicting complex LULC classes (Hyandye and Martz 2017; Irwin et al. 2009; Singh et al. 2015). This study adopted the CA-Markov model to predict LULC changes in the year 2050 for Erbil governorate based on the (1988–2002) and (2002–2017) LULC maps produced from the maximum likelihood classification (Fig. 2). This was accomplished in two steps; firstly, the Markov model was used to generate transition probability matrices of areas and hence conditional probability maps for (1988–2002) and (2002–2017) LULC maps respectively (Fig. 2). Model settings allowed only 15% proportional error for input images (i.e., with the maximum likelihood classification, assigning a proportional error of around 0.15 (15%) is recommended (Eric and Aldrik 2007; Takada et al. 2010). Secondly, using the probability of transition and conditional maps as input to the CA-Markov model, a 2017 LULC map was simulated. This map was then validated with the actual 2017 LULC map as a necessary step to calibrate the model (section 2.5.3.1). After model validation, a LULC map for 2050 was modelled from the existing (2002–2017) maps. In the Markov-CA modelling for the 2017 and 2050, model settings of 5 × 5 grid-cell contiguity filter and 11 iterations of cellular automata within the IDRISI 17.0. were used (Sang et al. 2011; Takada et al. 2010).

Model validation

Before modelling the LULC map for 2050, it was necessary to validate the model output. The validation was accomplished by using a time window of the classified data as reference data (classified 2017 LULC map) against the 2017 modelled LULC map. An embedded VALIDATE module in IDRISI 17.0. was used to compare the degree of agreements between the modelled and the classified map. The agreement indices are based on the standard Kappa Index of Agreement (KIA) with some spatial correlation variations. These variations, namely include; Kappa for locationStrata ($K_{locationStrata}$), for location ($K_{location}$), for no information (K_{no}), and Kappa standard ($K_{standard}$) (Pontius Jr 2002; Pontius Jr and Millones 2011; Pontius 2000). The K location and locationSrata indicate the accuracy of spatial dimensions of the quantity and locations of the grid-cells of a certain class category of the LULC maps. Kno indicates the general agreement between proportions of the reference and modelled maps, regardless of having information on the quantity and location of certain class categories. K standard refers to the proportion of correctly correlating a class category against the ones that correlated correctly by chance. The Kappa values for these variations range between 0 and 1 (0% and 100%); the closer the value to 100%, the better is the accuracy of the agreement (Christensen and Jokar Arsanjani 2020).

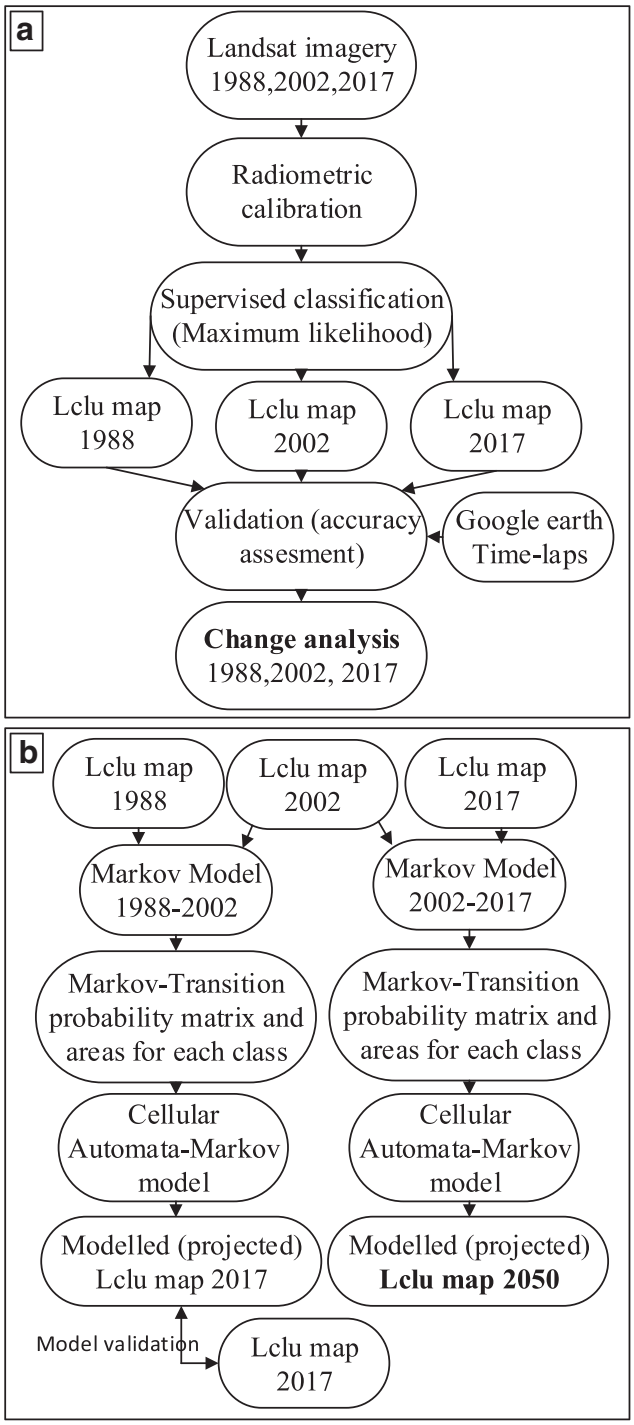

Fig. 2 Research workflow

Table 3 Error matrix for the year 1988

Class	Dv	Sv	ALa	Afa	Pla	BLa	BaL	Wa	Total	User Accuracy
Dv	54.00	0.00	0.00	0.00	6.00	0.00	0.00	0.00	60.00	0.90
Sv	0.00	56.00	1.00	2.00	0.00	0.00	1.00	0.00	60.00	0.93
ALa	1.00	6.00	52.00	1.00	0.00	0.00	0.00	0.00	60.00	0.87
Afa	0.00	0.00	1.00	51.00	0.00	4.00	4.00	0.00	60.00	0.85
Pla	8.00	0.00	0.00	0.00	52.00	0.00	0.00	0.00	60.00	0.87
BLa	0.00	0.00	0.00	6.00	0.00	54.00	0.00	0.00	60.00	0.90
BaL	0.00	1.00	0.00	5.00	0.00	0.00	54.00	0.00	60.00	0.90
Wa	0.00	0.00	3.00	1.00	0.00	0.00	0.00	56.00	60.00	0.93
Total	63.00	63.00	57.00	66.00	58.00	58.00	59.00	56.00	480.00	0.00
Producer Accuracy	0.86	0.89	0.91	0.77	0.90	0.93	0.92	1.00	0.00	0.89
Kappa	0.88									

Key: Dv (Dense Vegetation) Sv (Sparse Vegetation) ALa (Agricultural Land) Afa (Agricultural Fallow) Pla (Plantation) BLa (Built-up Area) BaL (Barren Land) Wa (Waterbody)

Results and discussion

Classification assessment and change analysis

For accuracy assessment of the maximum likelihood classification, error matrices for the target years were established (Tables 3, 4 and 5). The overall Kappa index of the agreement for the three consecutive years; 1988, 2002, and 2017 were 0.88 (88%), 0.95 (95%), 0.92(92%), respectively. The user's and producer's accuracies as per class category were in the range of 0.77 (77%) and 1.00 (100%) (Tables 3, 4 and 5). These values indicate that the number of pixels correctly classified in proportion to classified pixels by chance was much higher. Thus the LULC maps can reliably be used for change analysis and prediction (Anderson 1976). Employing the Google Earth Historical Imagery significantly assisted the process of classification accuracy assessment. However, local knowledge on the study area's physiography was also useful in accurately extracting class categories. Overall, eight class categories were identified from the satellite imagery, which were acquired during early and late July of 1988, 2002, and 2017. The time of image acquisition may play a role in defining the class category quantity.

Change statistics demonstrated between 1988 and 2002, the dense vegetation, agricultural fallow, plantation, built-up land, and water bodies have increased by 3.8%, 1.2%, 0.2%, 0.1%, and 0.1%, respectively (Table 6). These changes are proportional with respect to the whole land cover types between the two-time-period. The increase in the built-up area for 14 years (1988–2002) is not quite significant, yet one may

Table 4 Error matrix for the year 2002

Class	Dv	Sv	ALa	Afa	Pla	BLa	BaL	Wa	Total	User Accuracy
Dv	59.00	0.00	1.00	0.00	0.00	0.00	0.00	0.00	60.00	0.98
Sv	0.00	58.00	2.00	0.00	0.00	0.00	0.00	0.00	60.00	0.97
ALa	0.00	0.00	60.00	0.00	0.00	0.00	0.00	0.00	60.00	1.00
Afa	0.00	0.00	0.00	55.00	0.00	3.00	0.00	2.00	60.00	0.92
Pla	5.00	0.00	0.00	0.00	55.00	0.00	0.00	0.00	60.00	0.92
BLa	0.00	0.00	0.00	0.00	0.00	60.00	0.00	0.00	60.00	1.00
BaL	0.00	0.00	0.00	4.00	0.00	0.00	56.00	0.00	60.00	0.93
Wa	0.00	0.00	3.00	3.00	0.00	0.00	0.00	54.00	60.00	0.90
Total	64.00	58.00	66.00	62.00	55.00	63.00	56.00	56.00	480.00	0.00
Producer Accuracy	0.92	1.00	0.91	0.89	1.00	0.95	1.00	0.96	0.00	0.95
Kappa	0.95									

Key: Dv (Dense Vegetation) Sv (Sparse Vegetation) ALa (Agricultural Land) Afa (Agricultural Fallow) Pla (Plantation) BLa (Built-up Area) BaL (Barren Land) Wa (Waterbody)

Table 5 Error matrix for the year 2017

Class	Dv	Sv	ALa	Afa	Pla	BLa	BaL	Wa	Total	User Accuracy
Dv	56.00	0.00	0.00	0.00	4.00	0.00	0.00	0.00	60.00	0.93
Sv	0.00	50.00	10.00	0.00	0.00	0.00	0.00	0.00	60.00	0.83
ALa	0.00	0.00	57.00	3.00	0.00	0.00	0.00	0.00	60.00	0.95
Afa	0.00	0.00	0.00	57.00	0.00	0.00	3.00	0.00	60.00	0.95
Pla	4.00	0.00	0.00	0.00	56.00	0.00	0.00	0.00	60.00	0.93
BLa	0.00	0.00	0.00	0.00	0.00	56.00	4.00	0.00	60.00	0.93
BaL	0.00	0.00	0.00	1.00	0.00	2.00	57.00	0.00	60.00	0.95
Wa	0.00	0.00	0.00	1.00	0.00	0.00	0.00	59.00	60.00	0.98
Total	60.00	50.00	67.00	62.00	60.00	58.00	64.00	59.00	480.00	0.00
Producer Accuracy	0.93	1.00	0.85	0.92	0.93	0.97	0.89	1.00	0.00	0.93
Kappa	0.92									

Key: Dv (Dense Vegetation) Sv (Sparse Vegetation) ALa (Agricultural Land) Afa (Agricultural Fallow) Pla (Plantation) BLa (Built-up Area) BaL (Barren Land) Wa (Waterbody)

consider that the economic and the political situations were not stable during that period. In 1988 the eight years of the Iran-Iraq war just ceased, and after that, in 1991, the gulf war was started and followed by the United Nations (UN) economic sanctions. The increase in agricultural fallow may refer to limited agricultural activity by farmers in 2002, or the land has already been harvested. The increase in the dense vegetation and plantation in the remote mountainous areas (e.g., Choman, Soran, and Mergasur), both in density and in magnitude, can be noticed (Fig. 5). Surprisingly, the water bodies increased by 0.1% (from 9.6 km^2 to 21.9 km^2), most likely due to fish farming activity and the establishing some small and moderate scale artificial reservoirs. In contrast, sparse vegetation, agricultural land, and barren land have decreased by 2.7%, 0.1%, 2.6%, respectively. Spare vegetation (Table 6) is mostly composed of thin forest and oak tree shrubland (Khwarahm 2020). Over time some of these classes change in structure, for example, change to dense vegetation. The same argument is likely accurate to agriculture and barren lands, for example, barren land changed to a built-up area or the plantation.

Between the period 2002–2017, change statistics demonstrated dense vegetation, barren land, and water bodies have reduced by −2.4%, 10.2%, and 0.1%, respectively. In contrast, the built-up area and agricultural fallow increased by 2.3% and 8.6%, respectively. During that period, a significant area of barren land was exploited for agricultural activity; thus, it reduced by around 10% (from 10,953.7 km^2 to 9463.9 km^2) (Table 6). Aftermath of the Iraq invasion in 2003 by the USA and the coalition forces brought foreign aids and investment into the region. For example, reviving the agricultural sector

Table 6 Change analysis: Area and percentage of the land cover land use classes

	1988		2002		2017		2017_ Modelled		2050_Modelled	
Class	Area_km^2	Area %	Area_km^2	Area %	Area_km^2	Area %	Area_km^2	Area %	Area_km^2	Area %
Dv	156.8	1.1	706.5	4.9	367.2	2.5	625	4.3	546.9	3.8
Sv	2539.5	17.5	2154.0	14.8	2274.6	15.6	2829.3	19.4	2052.8	14.1
ALa	128.6	0.9	115.4	0.8	230.0	1.6	220.4	1.5	412.9	2.8
Afa	277.4	1.9	453.4	3.1	1705.7	11.7	791.5	5.4	2507.7	17.2
Pla	29.8	0.2	60.9	0.4	70.8	0.5	64.8	0.4	120	0.8
BLa	73.6	0.5	81.2	0.6	424.1	2.9	113.3	0.8	1160.8	8.0
BaL	11,331.7	77.9	10,953.7	75.3	9463.9	65.1	9880.9	67.9	7721.0	53.1
Wa	9.6	0.1	21.9	0.2	10.7	0.1	21.8	0.1	24.9	0.2
Total	14,547	100	14,547	100	14,547	100	14,547	100	14,547	100

Key: Dv (Dense Vegetation) Sv (Sparse Vegetation) ALa (Agricultural Land) Afa (Agricultural Fallow) Pla (Plantation) BLa (Built-up Area) BaL (Barren Land) Wa (Waterbody)

Table 7 Coefficients of agreement between the actual LULC map 2017 and modelled 2017 LULC map

Classification agreement/disagreement			
According to the ability to specify accurately quantity and allocation			
Information of Quantity			
Information of Allocation	No[n]	Medium[m]	Perfect[p]
Perfect[P(x)]	P(n) = 0.3753	P(m) = 0.9477	P(p) = 1.0000
Perfect Stratum[K(x)]	K(n) = 0.3753	K(m) = 0.9477	K(p) = 1.0000
Medium Grid[M(x)]	M(n) = 0.3195	M(m) = 0.8523	M(p) = 0.8658
Medium Stratum[H(x)]	H(n) = 0.1111	H(m) = 0.4114	H(p) = 0.4046
No[N(x)]	N(n) = 0.1111	N(m) = 0.4114	N(p) = 0.4046
Agreement Chance = 0.1111			
Agreement Quantity = 0.3003			
Agreement Gridcell = 0.4409			
Disagree Gridcell = 0.0953			
Disagree Quantity = 0.0523			
Kno = 0.8339			
Klocation = 0.8222			
KlocationStrata = 0.8222			
Kstandard = 0.7491			

and building/rebuilding infrastructure may have contributed to these changes.

In the period between 1988 and 2017, contrary to the built-up area, barren land showed a steady decrease of around 13% of the total area, whereas the built-up area increased from 73.6 km^2 to 424.1km^2 (Table 6). The increase in the area of a built-up area refers to increasing the population and development of infrastructure (Pandey and Khare 2017). One of the main drivers that trigger LULC changes is population growth (Berihun et al. 2019). Iraq and KRI, like the rest of the Middle East, have seen significant population growth and partial economic growth in the last two decades. For example, in Iraq, the population has increased from ~12.46 million to ~38.275 in just four decades (i.e., an increase by 308% between 1977 to 2017) (UN 2017).

Model validation

The modelled LULC map of 2017 generated by CA-Markov model based on the historical status of 1988–2002 was validated by the actual LULC map of 2017 produced from the satellite images. Overall, there was a significant level of agreement between the modelled and actual LULC maps (Table 7). The overall Kappa statistical variations of $K_{no} = 0.8339$, $K_{location} = 0.8222$, $K_{locationStrata} = 0.8222$, $K_{standard} = 0.7491$ were achieved. These values are considered acceptable as far as the reliability of model validation is concerned for further use (Landis and Koch 1977; Pontius Jr and Millones 2011). The model performed satisfactorily in predicting the water bodies, barren land, agricultural land, plantation, and sparse vegetation (Table 6). However, it has overestimated the dense

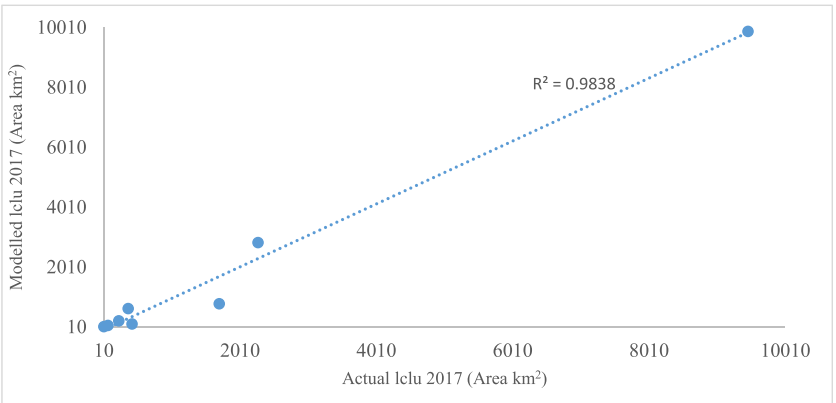

Fig. 3 Linear trend line indicating the relationship between the actual and predicted (modelled) LULC maps of 2017

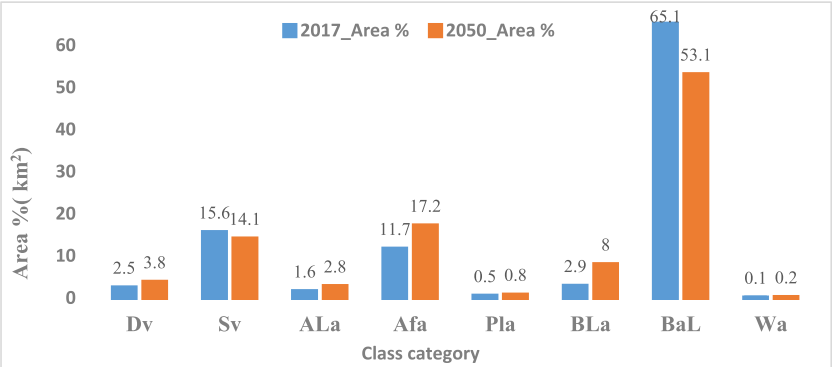

Fig. 4 Area percentage (%) of changes per class category between 2017 and 2015

vegetation by 1.8% of the actual area (367.2 km^2). In contrast, it has underestimated the agricultural fallow and built-up area by 6.3% (1705.7) and 2.1% (424.1 km^2) of the actual area, respectively. The underestimation, most likely caused by the disagreement quantity value (Table 7), which in turn has slightly affected the overall performance of the model. Furthermore, the source of the difference between the classified LULC map of 2017 and the modelled map of 2017 was likely to come from underestimating some class categories, particularly agricultural fallow and built-up area (Table 7). The underestimation, most likely caused by the input data (i.e., LULC maps of 1988 and 2002). Because there is an obvious time difference between 2002 and 2017, during which the pace and quantity of LULC change dynamic were apparently different compared to the period between 1988 and 2002. However, the overall performance of the model in simulating a future scenario based on the transition probability matrix of 1988–2002 demonstrated decent accuracy (Table 7 and Fig. 3). Previous studies have reported various values of Kappa coefficient variation for CA-Markov model. For example, Hyandye and Martz (2017) and Singh et al. (2018) reported the $K_{standard}$ of 0.68 and 0.59, respectively. Others have reported values of 0.88 (Rimal et al. 2017) and 0.95 (Munthali et al. 2020). The model capability of simulating near-perfect scenario from predefined inputs partly depends on the contiguity filter number (i.e., 5X5 filter and 10X10 performance), the suitability maps (Verburg et al. 2008), and probably the type of classifier used for input data classification. Furthermore, the overall model settings, for example, cellular automata iteration and various validation techniques, probably should be considered.

Table 8 Shows the probability of transition % (class change) from 2017 to 2050

Class	Dv	Sv	ALa	Afa	Pla	BLa	BaL	Wa
Dv	0.835	0.077	0.000	0.000	0.085	0.003	0.000	0.000
Sv	0.069	0.807	0.005	0.000	0.000	0.000	0.118	0.000
ALa	0.001	0.000	0.792	0.142	0.000	0.006	0.055	0.004
Afa	0.001	0.000	0.038	0.827	0.001	0.023	0.110	0.000
Pla	0.004	0.021	0.152	0.000	0.823	0.000	0.000	0.000
BLa	0.001	0.003	0.145	0.000	0.000	0.850	0.000	0.002
BaL	0.000	0.063	0.013	0.093	0.000	0.011	0.820	0.000
Wa	0.001	0.008	0.101	0.041	0.000	0.000	0.000	0.849

Correlation between actual and modelled LULC

Even though IDRISI 17.0. has an embedded VALIDATE module, which allows validating the modelled map with a reference map by executing various Kappa statistical variations; representing the agreement and disagreement degrees between corresponding class categories based on both quality and quantity (Table 7). Moreover, area-wise, the overall relationship between the modelled and classified maps, demonstrated the co-efficient of determination value of ($R^2 = 0.9838$) (Fig. 3). This result concurs with the study of Akbar et al. (2019), which reported the $R^2 = 0.90$ between actual and modelled LULC maps.

LULC change modelling

To accomplish the second main objective of this study, the produced LULC maps for the 1988–2002 and 2002–2017 were used to model 2017 and 2050 LULC maps, respectively. Future predictions demonstrate between 2017 and 2050, built-up area, agricultural land, plantation, dense vegetation, agricultural fallow and water body will increase by 173.7% (from 424.1 to 1160.8 km^2), 79.5% (from 230 to 412.9 km^2), 70.2%, (from 70.2 to 119.5 km^2), 48.9% (from 367.2–546.9 km^2), 47% (from 1705.7- 2507.7 km^2) and 132.7% (from 10.7 to 24.9 km^2), respectively. In contrast, sparse vegetation and barren land will decrease by 9.8%, (2274.6 to 2052.8 km^2), 18.4% (9463.9 to 7721.0 km^2), respectively (Table 6 and Fig. 4). These increases and decreases are proportional changes in respect to LULC class categories. In other words, the 173.7% increase in the built-up area in 2050 will be at the cost of reducing the area of other class categories. Moreover, changes in the areas (%) per class category from the period 2017 to 2050 indicated that the most dynamic class cover types were agricultural land, agricultural fallow,

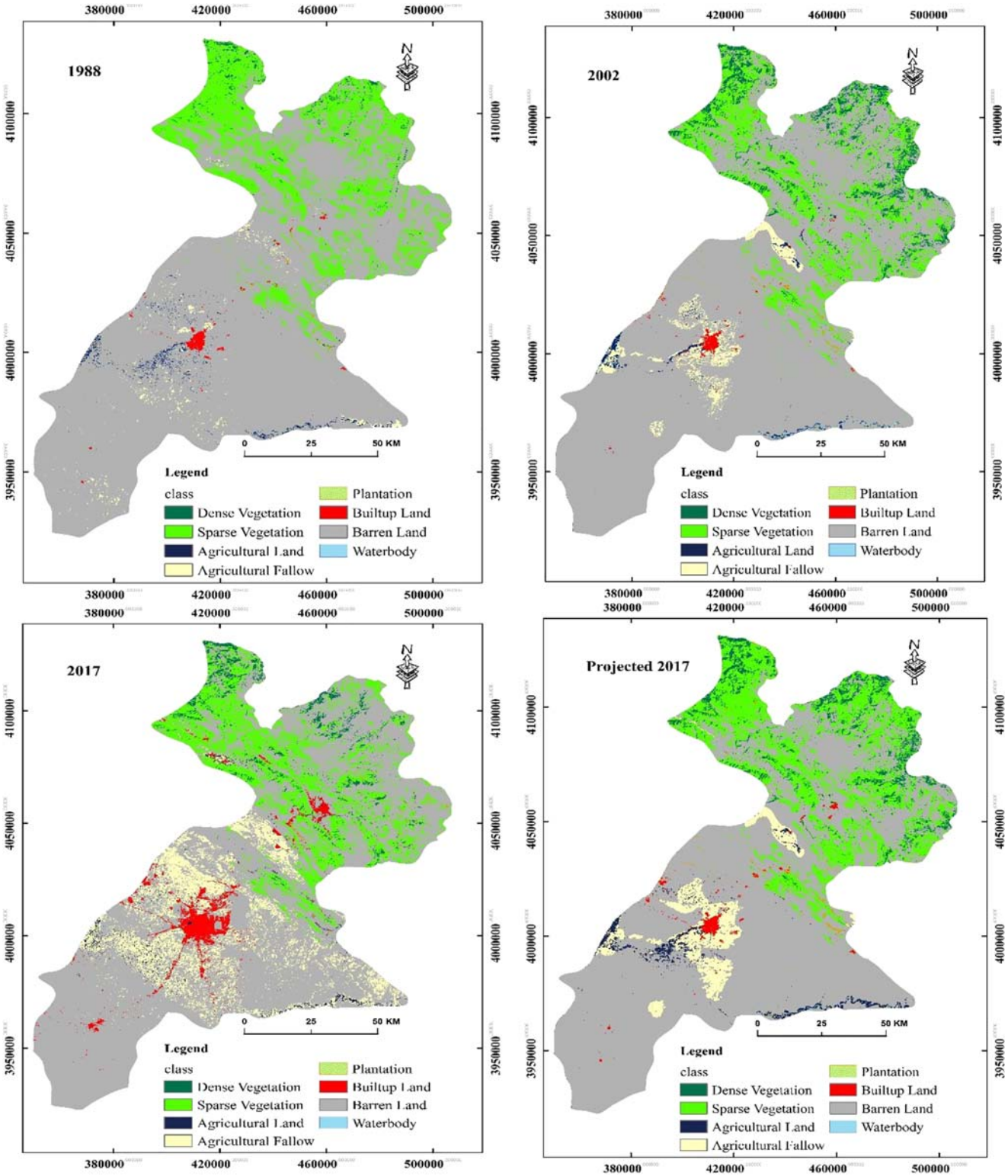

Fig. 5 LULC maps for a) 1988, b) 2002, c) 2007, and d) modelled 2017

barren land, and built-up area. The least dynamic cover types were dense vegetation, sparse vegetation, and water bodies. In 2050, the area of the water body will increase by only 1%, whereas the built-up area by more than 5% with respect to other cover types (Fig. 4). The most significant change that balance out the overall dynamic of the class categories will be the barren land. This class category comprises a remarkable area in comparison to the classes.

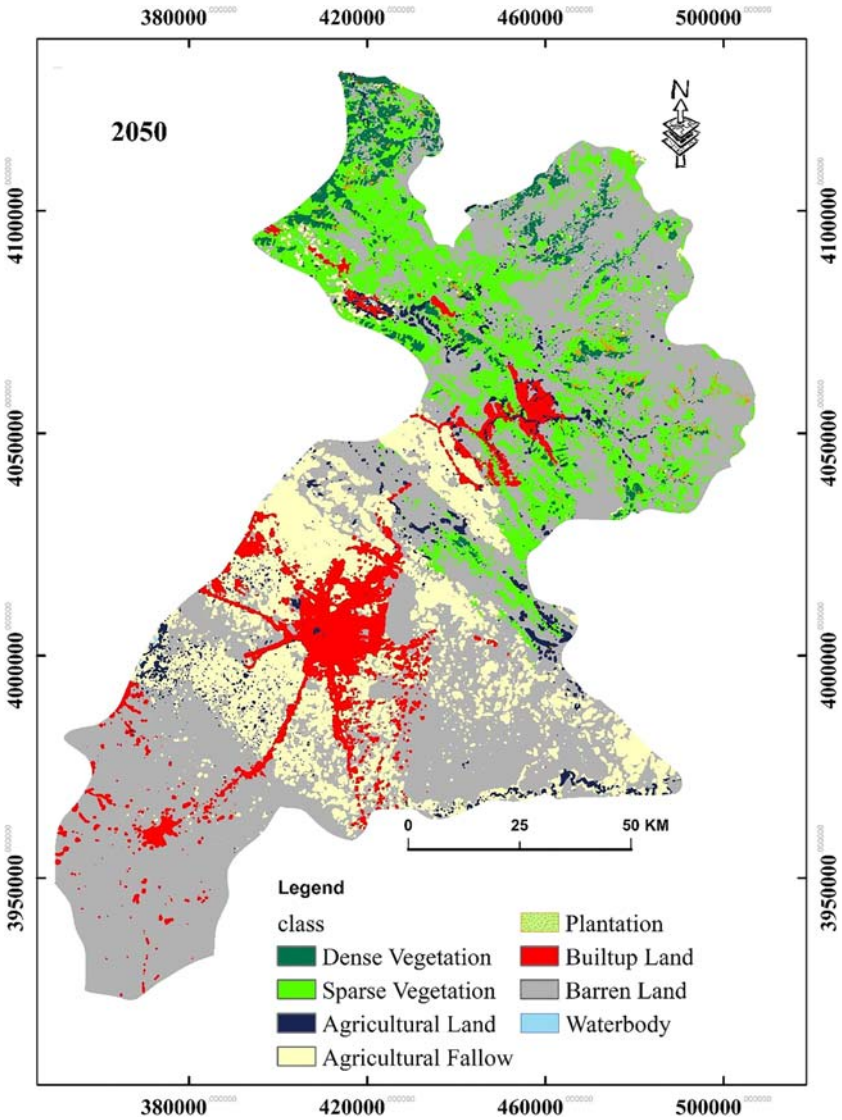

Fig. 6 The modelled land cover land use status of Erbil governorate for the year 2050

The trend of changes in the class categories seemed to be linear, and they will further grow linear in the future. Linear positive or negative trend changes together with the spatial direction provide useful information on the pace and dynamic of transformation. This information is useful in environmental management and understanding ecosystems' function comprehensively (Dewan and Yamaguchi 2009) (Fig. 4).

The proportionality of transition or changes from one class category to another in the study area is surprisingly in balance (Table 8). The transition probability matrix between 2017 and 2050 indicated that (16.5%) of dense vegetation would change to the built-up area, plantation, and sparse vegetation; the remainder stays as it is. Sparse vegetation predominantly will change by 19.2% to dense vegetation and agricultural land. Similarly, around 14.6% of agricultural land will mostly change to agricultural fallow and water bodies (Table 8). The majority of the changed portion of barren land will change to built land and agricultural land by around 1.1% and 9.5% of agriculture, respectively. Counterintuitively, 14.2% of water bodies will change to agricultural land (etc., active and fallow). In other words, this result indicates that some areas, which were covered by water bodies in 2017, will be replaced by agricultural lands and, in turn, other water bodies will emerge. The emergence of water bodies will be most probably be in the form of catchments and small scale reservoirs from fishery activities (Figs. 5 and 6).

Conclusions

Erbil governorate is one of the major governorates in the Republic of Iraq, which includes seven administrative districts, and it isthe political and economic capital of the KRI in the north of Iraq. This region is considered one of the vital

biodiversity hot spots in Iraq (Zohary 1973). The landscape of the area has been changing at a linear pace, particularly in the past 15 years. Developing techniques to measure spatially past, current, and future changes provide invaluable information for decision-makers, biodiversity conservationists, and assist in identifying ecologically degraded areas concerning the landscape's total mosaic. This study has used integrated systems of remote sensing, GIS, and earth surface modeller (CA-Markov) to predict the future dynamics of LULC class categories in 2050 for Erbil governorate. GIS and remote sensing provide a unique opportunity to monitor and quantify LULC changes over space and time consistently.

There have been significant LULC changes specifically to urban development (i.e., built-up area) since 1988 in Erbil city, particularly in the vicinity of the main roads and towards, west, south-east, and south-west of the city. Province-wise in the south of the city, Makhmur district and the north Shaqlawa and Soran will see significant urban growth in 2050. Nevertheless, these developments will come at the cost of other landscape fabrics, for example, agricultural land and barren land.

Future predictions demonstrate that between 2017 and 2050, built-up land, agricultural land, plantation, dense vegetation and water body will increase by 173.7%, 79.5%, 70.2%, 48.9% and 132.7%, respectively. In contrast, sparse vegetation, barren land will decrease by 9.7%, 18.4%, respectively. Barren lands and spare vegetation are equally important habitats for various plant and animal species. For example, birds (See-see Partridge *Ammoperdix griseogularis*, Black-headed Bunting *Emberiza melanocephala*, Eastern Black-eared Wheatear *Oenanthe melanoleuca*, and Finsch's Wheatear *Oenanthe finschii*), plants (*Quercus spp*., *Prunus spp*., and *Pistachio eurocarpa* and genus *Astragalus*); and mammals (Golden Jackal *Canis aureus*, Red Fox *Vulpes vulpes*, Grey Wolf *Canis lupus*, and Bezoar Ibex *Capra aegagrus*). Current and future exploitation of the LULC should take into account the significance of these endemic species to the region as far as the conservation effort of biodiversity is concerned.

The transition probability matrix indicated that (16.5%) of dense vegetation would change to the built-up area, plantation, and sparse vegetation. Sparse vegetation predominantly will change by 19.2% to dense vegetation and agricultural land. Similarly, around 14.6% of agricultural land will mostly change to agricultural fallow and water bodies (Table 8). Portions of barren land will change to built land and agricultural land by around 1.1% and 9.5%, respectively.

The study outputs provide robust baseline information for future exploitation of the land surface features with less impact on biodiversity and landscape integrity. The 2050 map can confidently be used as a benchmark for decision making, planning, sustainable management of the natural environment, and biodiversity conservation.

Acknowledgements The authors would like to express their gratitude to the United States Geological Survey to make the Earth Observation data available. We would also like to thank Mr. Shakawan Hussain from Erbil University for his assistance and support.

Data availability Not applicable

Compliance with ethical standards

Conflicts of interest/competing interests Not applicable

Code availability Not applicable

References

Akbar TA, Hassan QK, Ishaq S, Batool M, Butt HJ, Jabbar H (2019) Investigative spatial distribution and modelling of existing and future urban land changes and its impact on urbanization and economy. Remote Sens 11:105

Alkaradaghi K, Ali SS, Al-Ansari N, Laue J (2018) Evaluation of land use & land cover change using multi-temporal landsat imagery: a case study Sulaimaniyah governorate, Irag. J Geogr Inf Syst 10: 247–260

Anderson JR (1976) A land use and land cover classification system for use with remote sensor data vol 964. US Government Printing Office

Berihun ML, Tsunekawa A, Haregeweyn N, Meshesha DT, Adgo E, Tsubo M, Masunaga T, Fenta AA, Sultan D, Yibeltal M (2019) Exploring land use/land cover changes, drivers and their implications in contrasting agro-ecological environments of Ethiopia. Land Use Policy 87:104052

Biswas M, Banerji S, Mitra D (2019) Land-use–land-cover change detection and application of Markov model: a case study of eastern part of Kolkata environment. Dev Sustain:1–20

Butt A, Shabbir R, Ahmad SS, Aziz N (2015) Land use change mapping and analysis using remote sensing and GIS: a case study of Simly watershed, Islamabad, Pakistan. Egypt J Remote Sens Space Sci 18: 251–259

Christensen M, Jokar Arsanjani J (2020) Stimulating implementation of sustainable development goals and conservation action: predicting future land use/cover change in Virunga National Park, Congo. Sustainability 12:1570

Congalton RG, Green K (2019) Assessing the accuracy of remotely sensed data: principles and practices. CRC Press

Dewan AM, Yamaguchi Y (2009) Land use and land cover change in greater Dhaka, Bangladesh: Using remote sensing to promote sustainable urbanization. Appl Geogr 29:390–401

Eastman JR (2003) IDRISI Kilimanjaro: Guide to GIS and image processing. Clark University, Worcester

Eastman J (2012) IDRISI Selva: guide to GIS and image processing Clark Labratories. Clark University, Worcester

Eric K, Aldrik B (2007) Modelling land-use change: progress and applications. Springer, The Netherlands

Faqe Ibrahim G (2017) Urban land use land cover changes and their effect on land surface temperature: case study using Dohuk City in the Kurdistan Region of Iraq. Climate 5:13

Foody GM (2002) Status of land cover classification accuracy assessment. Remote Sens Environ 80:185–201

Fu X, Wang X, Yang YJ (2018) Deriving suitability factors for CA-Markov land use simulation model based on local historical data. J Environ Manag 206:10–19

Gibson GR, Campbell JB, Zipper CE (2015) Sociopolitical influences on cropland area change in Iraq, 2001–2012. Appl Geogr 62:339–346

Gómez C, White JC, Wulder MA (2016) Optical remotely sensed time series data for land cover classification: a review. ISPRS J Photogramm Remote Sens 116:55–72

Guan D, Li H, Inohae T, Su W, Nagaie T, Hokao K (2011) Modeling urban land use change by the integration of cellular automaton and Markov model. Ecol Model 222:3761–3772

Guest E (1966) Flora of Iraq. Volume 1, introduction to the flora: an account of the geology, soils, climate and ecology of Iraq with gazetteer, glossary and bibliography. Ministry of Agriculture

Hadeel A, Jabbar MT, Chen X (2010) Environmental change monitoring in the arid and semi-arid regions: a case study Al-Basrah Province, Iraq. Environ Monit Assess 167:371–385

Hadi SJ, Shafri HZ, Mahir MD (2014) Modelling LULC for the period 2010-2030 using GIS and remote sensing: a case study of Tikrit, Iraq. In: IOP conference series: earth and environmental science, 2014, vol 1. IOP Publishing, p 012053

He D, Zhou J, Gao W, Guo H, Yu S, Liu Y (2014) An integrated CA-markov model for dynamic simulation of land use change in Lake Dianchi watershed Beijing. Daxue Xuebao (Ziran Kexue Ban)/Acta Scientiarum Naturalium Universitatis Pekinensis 50:1095-1105

He C, Liu Z, Gou S, Zhang Q, Zhang J, Xu L (2019) Detecting global urban expansion over the last three decades using a fully convolutional network. Environ Res Lett 14:034008

Hishe S, Bewket W, Nyssen J, Lyimo J (2020) Analysing past land use land cover change and CA-Markov-based future modelling in the middle Suluh Valley, Northern Ethiopia. Geocarto Int 35:225–255

Hooke RL, Martín-Duque JF, Pedraza J (2012) Land transformation by humans: a review. GSA Today 22:4–10

Houet T, Hubert-Moy L (2006) Modelling and projecting land-use and land-cover changes with a cellular automaton in considering landscape trajectories: an improvement for simulation of plausible future states. EARSel eProceedings 5(1):63–76

Hyandye C, Martz LW (2017) A Markovian and cellular automata land-use change predictive model of the Usangu Catchment. Int J Remote Sens 38:64–81

Irwin EG, Jayaprakash C, Munroe DK (2009) Towards a comprehensive framework for modeling urban spatial dynamics. Landsc Ecol 24: 1223–1236

Jensen JR (1996) Introductory digital image processing: a remote sensing perspective, vol Ed. 2. Prentice-Hall Inc.

Kamusoko C, Aniya M, Adi B, Manjoro M (2009) Rural sustainability under threat in Zimbabwe–simulation of future land use/cover changes in the Bindura district based on the Markov-cellular automata model. Appl Geogr 29:435–447

Karki S, Thandar AM, Uddin K, Tun S, Aye WM, Aryal K, Kandel P, Chettri N (2018) Impact of land use land cover change on ecosystem services: a comparative analysis on observed data and people's perception in Inle Lake, Myanmar. Environ Syst Res 7:25

Khwarahm NR (2020) Mapping current and potential future distributions of the oak tree (Quercus aegilops) in the Kurdistan Region. Iraq Ecological Processes 9:1–16

Lambin EF, Meyfroidt P (2011) Global land use change, economic globalization, and the looming land scarcity. Proc Natl Acad Sci 108: 3465–3472

Landis JR, Koch GG (1977) The measurement of observer agreement for categorical data. Biometrics 33:159–174

Li W, Dong R, Fu H, Wang J, Yu L, Gong P (2020) Integrating Google earth imagery with Landsat data to improve 30-m resolution land cover mapping. Remote Sens Environ 237:111563

Liang S, Fang H, Morisette JT, Chen M, Shuey CJ, Walthall CL, Daughtry CS (2002) Atmospheric correction of Landsat ETM+ land surface imagery. II Validation and applications. IEEE Trans Geosci Remote Sens 40:2736–2746

Liping C, Yujun S, Saeed S (2018) Monitoring and predicting land use and land cover changes using remote sensing and GIS techniques—a case study of a hilly area, Jiangle, China. PLoS ONE 13

López E, Bocco G, Mendoza M, Duhau E (2001) Predicting land-cover and land-use change in the urban fringe: a case in Morelia city, Mexico. Landsc Urban Plan 55:271–285

Mohammed EA, Hani ZY, Kadhim GQ (2018) Assessing land cover/use changes in Karbala city (Iraq) using GIS techniques and remote sensing data. In: Journal of Physics: Conference Series, 2018. vol 1. IOP Publishing, p 012047

Muller MR, Middleton J (1994) A Markov model of land-use change dynamics in the Niagara region, Ontario, Canada. Landsc Ecol 9: 151–157

Munthali M, Mustak S, Adeola A, Botai J, Singh S, Davis N (2020) Modelling land use and land cover dynamics of Dedza district of Malawi using hybrid Cellular Automata and Markov model. RSASE 17:100276

Naboureh A, Moghaddam MHR, Feizizadeh B, Blaschke T (2017) An integrated object-based image analysis and CA-Markov model approach for modeling land use/land cover trends in the Sarab plain. Arab J Geosci 10:259

Omar NQ, Ahamad MSS, Hussin W, Samat N (2014) Modelling land-use and land-cover changes using Markov-CA, and multiple decision making in Kirkuk city. IJSRES 2:29–42

Pandey BK, Khare D (2017) Analyzing and modeling of a large river basin dynamics applying integrated cellular automata and Markov model. Environ Earth Sci 76:779

Parsa VA, Yavari A, Nejadi A (2016) Spatio-temporal analysis of land use/land cover pattern changes in Arasbaran Biosphere Reserve: Iran. Modeling Earth Syst Environ 2:1–13

Pflugmacher D, Rabe A, Peters M, Hostert P (2019) Mapping pan-European land cover using Landsat spectral-temporal metrics and the European LUCAS survey. Remote Sens Environ 221:583–595

Pontius RG (2000) Quantification error versus location error in comparison of categorical maps. Photogramm Eng Remote Sens 66:1011–1016

Pontius RG Jr (2002) Statistical methods to partition effects of quantity and location during comparison of categorical maps at multiple resolutions. Photogramm Eng Remote Sens 68:1041–1050

Pontius RG Jr, Cheuk ML (2006) A generalized cross-tabulation matrix to compare soft-classified maps at multiple resolutions. Int J Geogr Inf Sci 20:1–30

Pontius RG Jr, Millones M (2011) Death to Kappa: birth of quantity disagreement and allocation disagreement for accuracy assessment. Int J Remote Sens 32:4407–4429

Qader SH, Dash J, Atkinson PM, Rodriguez-Galiano V (2016) Classification of vegetation type in Iraq using satellite-based phenological parameters. IEEE J Sel Top Appl Earth Obs Remote Sens 9: 414–424

Regmi R, Saha S, Subedi D (2017) Geospatial analysis of land use land cover change modeling in Phewa lake watershed of Nepal by Using GEOMOD Model Himalayan Physics 65–72

Richards JA, Richards J (1999) Remote sensing digital image analysis vol 3. Springer

Rimal B, Zhang L, Keshtkar H, Wang N, Lin Y (2017) Monitoring and modeling of spatiotemporal urban expansion and land-use/land-cover change using integrated Markov chain cellular automata model. ISPRS Int J Geo Inf 6:288

Rosenfield GH (1986) Analysis of thematic map classification error matrices. Photogramm Eng Remote Sens 52:681–686

Sang L, Zhang C, Yang J, Zhu D, Yun W (2011) Simulation of land use spatial pattern of towns and villages based on CA–Markov model. Math Comput Model 54:938–943

Seto KC, Güneralp B, Hutyra LR (2012) Global forecasts of urban expansion to 2030 and direct impacts on biodiversity and carbon pools. Proc Natl Acad Sci 109:16083–16088

Singh SK, Mustak S, Srivastava PK, Szabó S, Islam T (2015) Predicting spatial and decadal LULC changes through cellular automata

Markov chain models using earth observation datasets and geo-information. Environ Process 2:61–78

Singh SK, Laari PB, Mustak S, Srivastava PK, Szabó S (2018) Modelling of land use land cover change using earth observation datasets of tons River Basin, Madhya Pradesh, India. Geocarto Int 33:1202–1222

Stehman SV, Czaplewski RL (1998) Design and analysis for thematic map accuracy assessment: fundamental principles. Remote Sens Environ 64:331–344

Takada T, Miyamoto A, Hasegawa SF (2010) Derivation of a yearly transition probability matrix for land-use dynamics and its applications. Landsc Ecol 25:561–572

Tolessa T, Senbeta F, Kidane M (2017) The impact of land use/land cover change on ecosystem services in the central highlands of Ethiopia. Ecosyst Serv 23:47–54

UN (2013) World Environment Day 2013: How environmental damage causes food insecurity in Iraq. https://reliefweb.int/sites/reliefweb.int/files/resources/Factsheet-WorldEnvironment-English.pdf. Accessed 31 Mar 2020

UN (2017) Department of economic and social affairs, population division . World population prospects: The 2017 revision, Volume II: Demographic Profiles. ST/ESA/SER.A/400

USDA (2008) Iraq: Drought reduces 2008/09 winter grain production. https://ipad.fas.usda.gov/highlights/2008/05/Iraq_may2008.htm. Accessed 30 Mar 2020

Van Oort P (2007) Interpreting the change detection error matrix. Remote Sens Environ 108:1–8

Verburg PH, Bakker M, Overmars KP, Staritsky I (2008) Landscape level simulation of land use change. In: Sustainability impact assessment of land use changes. Springer, pp 211–227

Wolfram S (1984) Cellular automata as models of complexity. Nature 311:419–424

Yang Q-s, Li X (2007) Integration of multi-agent systems with cellular automata for simulating urban land expansion Sci Geogr Sin 27:542

Zhu Z, Woodcock CE (2014) Continuous change detection and classification of land cover using all available Landsat data. Remote Sens Environ 144:152–171

Zohary M (1973) Geobotanical foundations of the Middle East. Gustav Fisher Verlag, Amsterdam